

# Quantum Computation for Pricing the Collateral Debt Obligations

Hao Tang,<sup>1,2,\*</sup> Anurag Pal,<sup>1,2</sup> Lu-Feng Qiao,<sup>1,2</sup> Tian-Yu Wang,<sup>1,2</sup> Jun Gao,<sup>1,2</sup> and Xian-Min Jin<sup>1,2,†</sup>

<sup>1</sup>*Center for Integrated Quantum Information Technologies (IQIT),*

*School of Physics and Astronomy and State Key Laboratory of Advanced Optical Communication Systems and Networks,  
Shanghai Jiao Tong University, Shanghai 200240, China*

<sup>2</sup>*CAS Center for Excellence and Synergetic Innovation Center in Quantum Information and Quantum Physics,  
University of Science and Technology of China, Hefei, Anhui 230026, China*

Collateral debt obligation (CDO) has been one of the most commonly used structured financial products and is intensively studied in quantitative finance. By setting the asset pool into different tranches, it effectively works out and redistributes credit risks and returns to meet the risk preferences for different tranche investors. The copula models of various kinds are normally used for pricing CDOs, and the Monte Carlo simulations are required to get their numerical solution. Here we implement two typical CDO models, the single-factor Gaussian copula model and Normal Inverse Gaussian copula model, and by applying the conditional independence approach, we manage to load each model of distribution in quantum circuits. We then apply quantum amplitude estimation as an alternative to Monte Carlo simulation for CDO pricing. We demonstrate the quantum computation results using IBM Qiskit. Our work addresses a useful task in finance instrument pricing, significantly broadening the application scope for quantum computing in finance.

Quantum computing for finance applications is an emerging field with quickly growing popularity. The finance industry involves various numerical and analytical tasks, *e.g.*, derivative pricing, credit rating, forex algorithm trading, and portfolio optimization, *etc.*. They all demand heavy quantitative work, and the improved calculation speed and precision would bring significant social value. Quantum computing aims at these very targets<sup>1</sup>. Early studies focused on improving finance models with basic quantum mechanics<sup>2-4</sup>. Schrodinger equations and Feynman's path integral were suggested to solve stochastic differential equations for pricing interest rate derivatives<sup>2</sup>, and Heisenberg uncertainty principle was used to interpret the leptokurtic and fat-tailed distribution of stock price volatilities<sup>4</sup>. Recent studies tend to utilize quantum advantages as a faster computing machine. Algorithms that can be implemented in quantum circuits, such as amplitude estimation<sup>5</sup>, quantum principle component analysis (PCA)<sup>6</sup>, quantum generative adversarial network (QGAN)<sup>7</sup>, the quantum-classical hybrid variational quantum eigensolver (VQE)<sup>8</sup> and quantum-approximate-optimization-algorithm (QAOA)<sup>9</sup>, spring up and begin to be applied to various financial quantitative tasks<sup>10-15</sup>.

Within all sectors of quantitative finance, the Monte-Carlo simulation always plays a significant role<sup>17-19</sup>, as only a few stochastic equations for derivative pricing have found analytical solutions<sup>20,21</sup>, while most can only be solved numerically by repeating random settings a great many times in an uncertainty distribution (*e.g.* normal or log-normal distribution), which therefore consumes much time. The quantum amplitude estimation (QAE) algorithm was raised<sup>5</sup> in 2002. It is newly suggested as a promising alternative to the Monte Carlo method, as it shows a quadratic speedup comparing to the latter<sup>10</sup>. So far, applications of QAE for option pricing<sup>11</sup> and credit risk analysis<sup>12</sup> have been demonstrated.

Considering the wide use of Monte Carlo simulation and the large variety of pricing models, the involvement of quantum techniques in finance is still at its infancy. Credit derivatives are frequently mentioned financial instruments because of the strong demand for tackling default risks in the finance industry. Collateral debt obligation (CDO) is a multi-name credit derivative backed on a pool of portfolios of defaultable assets (loans, bonds, credits *etc.*). CDO then packages the portfolio into several tranches with different returns and priorities to suffer the default loss<sup>19</sup>. CDO can effectively protect the senior tranche from the loss, but too many default events in the pool would still make the CDO collapsed, which was the case during the subprime financial crisis in 2008. Many voices were then made for improving the CDO pricing model and strengthening regulations in various aspects. Nonetheless, the CDO itself is a useful credit instrument that can work out and redistribute credit risks in a very quantitative way, and it is still widely studied in quantitative finance. So far, however, the implementation of complex credit instruments like CDO in quantum algorithms has never been reported.

In this work, we present the first quantum circuit implementation for CDO pricing using IBM Qiskit. To address the correlations among a large number of assets in the CDO pool, we use both the common Gaussian copula model<sup>22</sup> and an improved model, the Normal Inverse Gaussian copula model<sup>23,24</sup> that can interpret the skewness and kurtosis of the real markets which the Gaussian distribution cannot portray<sup>25-27</sup>. We follow a conditional independence approach to load the correlated distributions in the quantum circuits, and then use quantum comparators and QAE algorithm to calculate the losses in different tranches. We demonstrate the quantum computation results for a CDO that matches the classical

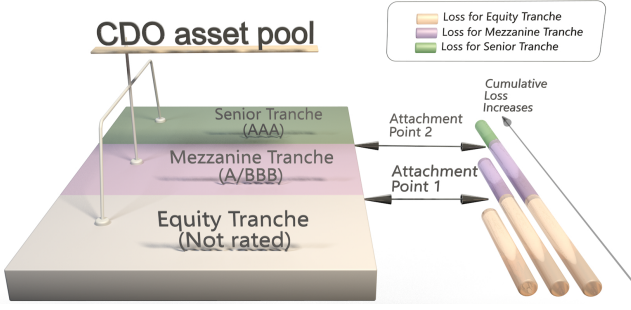


FIG. 1: **The CDO tranche structure.** The CDO comprises Equity Tranche (consisting of unrated or lowly rated securities), Mezzanine Tranche (consisting of intermediately rated securities) and Senior Tranche (consisting of highly rated securities), and the tranches have a sequence to bear the loss.

Monte Carlo method, suggesting a promising approach for pricing various derivatives.

## I. THE CDO STRUCTURE AND PRICING MODELS

### A. The CDO tranche structures

The CDO pool is normally divided into three tranches: the Equity, Mezzanine and Senior Tranche. As shown in Fig.1, when defaults occur, the Equity Tranche investors bear the loss first, then the Mezzanine Tranche investors if the loss is greater than the first attachment point. Only when the loss is greater than the second attachment point, will the Senior Tranche investors lose money. Therefore, Senior Tranche has the priority of receiving principle and interest payment, and the best protection from risk while having the lowest return.

Let  $K_{L_k}$  and  $K_{U_k}$  denote the lower and upper attachment point for Tranche  $k$ , respectively. When defaults occur, the buyer of the Tranche  $k$  will bear the loss in excess of  $K_{L_k}$ , and up to  $K_{U_k} - K_{L_k}$ . Let  $L$  denote the total loss for the portfolio and the loss suffered by the holders of Tranche  $k$  be  $L_k$ . As there are various default scenarios under some uncertainty distribution, we evaluate the expectation value of the tranche loss  $\mathbb{E}[L_k]$  for each Tranche  $k$ :  $\mathbb{E}[L_k] = \mathbb{E}[\min[K_{U_k} - K_{L_k}, \max(0, L - K_{L_k})]]$ . Then we can get the fair spread for this tranche denoted as  $r_k$ :

$$r_k = \frac{\mathbb{E}[L_k]}{N_k} = \frac{\mathbb{E}[L_k]}{K_{U_k} - K_{L_k}} \quad (1)$$

where  $N_k$  is the notional value of Tranche  $k$  of the portfolio, which can be calculated by  $K_{U_k} - K_{L_k}$ . To arrive at a fair price of a CDO, the return for investors of each tranche should be consistent with the expected loss the investors would bear. Therefore, such a fair spread is considered as the return for this tranche.

### B. The conditional independence approach

Usually the pool in CDO is a portfolio of correlated assets. Their default events are not independent, which can be modeled using the single-factor Gaussian copula.

Meanwhile, through years' practice on the Gaussian model, it is found not to well portray the phenomena in real CDO markets, *e.g.*, the 'correlation smile'<sup>25</sup>. In 2005, the Normal Inverse Gaussian (NIG) model was introduced to CDO pricing. In fact, price volatilities in derivative markets seldom show perfect Gaussian distribution. NIG can flexibly introduce a target skewness and kurtosis which the Gaussian model cannot achieve<sup>25-27</sup>. Explanation for NIG distribution and its probability density function (pdf) can be seen in Appendix I.

For either the Gaussian copula or NIG copula model, both of them can use the conditional independence approach<sup>28</sup> originally developed by Vašíček<sup>29,30</sup> for the multivariate distribution problems. Consider a portfolio that comprises  $n$  assets, each with a default risk  $X_i$ , and a correlation  $\gamma_i$  with the systematic risk  $Z$ . The mutually independent latent variables  $W_i$  can be used:  $W_i = \gamma_i Z + \sqrt{(1 - \gamma_i^2)} X_i$ , where  $\gamma_i$ s are correlation parameters that can be obtained by calibrating the market data. Let  $p_i^0$  be the original default probability for asset  $i$  that is uncorrelated to  $Z$ . Via detailed derivation<sup>28</sup>, the default probability under the influence of  $Z$  follows:

$$p_i(z) = F\left(\frac{F^{-1}(p_i^0) - \sqrt{\gamma_i}z}{\sqrt{1 - \gamma_i}}\right) \quad (2)$$

This Eq.(2) is derived for very general scenarios<sup>28</sup>.  $F$  stands for the distribution function of  $Z$ , which can be any continuous and strictly increasing distribution function, and in this content, they are Gaussian for the Gaussian copula model or NIG for the NIG copula model.  $F^{-1}$  stands for the inverse of distribution  $F$ .

Using this conditional independence model, given  $p_i(z)$  and  $\lambda_i$ , the loss that would incur for asset  $i$  when default happens, the expected total loss would be:

$$\mathbb{E}[L] = \int_{-\infty}^{\infty} \sum_{i=1}^n \lambda_i p_i(z) f(z) dz \quad (3)$$

where  $f(z)$  is the pdf for an uncertainty model. For Gaussian distribution with a variance  $\sigma$ , integrating  $z$  from  $-3\sigma$  to  $3\sigma$  would cover 99.73% of the distribution.

## II. QUANTUM CIRCUIT CONSTRUCTION

### A. Load the correlating default risks

To apply quantum computation for CDO pricing, the primary task is to load the default risk for each asset of the portfolio into the quantum circuit. Either the Gaussian or NIG model can be loaded in the circuit following

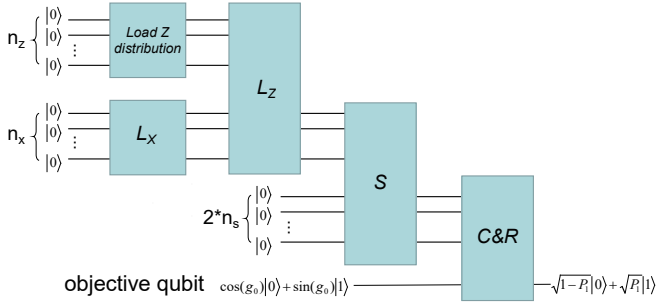


FIG. 2: **The quantum circuit framework.** The quantum circuit firstly uses operator  $\mathcal{L}_X$  to load the assets with non-correlated independent default risks, and then loads  $z$  distribution and uses operator  $\mathcal{L}_Z$  to address the correlation among asset default risks, and further sums up the total portfolio loss using operator  $\mathcal{S}$ . Then it comes to the comparator operator  $\mathcal{C}$  and the piecewise linear rotation operator  $\mathcal{R}$  to calculate the tranche loss, which is related to  $P_1$ , the probability of the objective qubit at the state  $|1\rangle$  after rotation.

a previous treatment<sup>12</sup> for the conditional independence model.

We firstly load the uncorrelated default events  $X_i$  ( $i = 1, 2, \dots, n$ ) using linear  $Y$ -rotation gate. The default probability  $p_i$  for each asset  $i$  can be obtained from its historical performance. The operator  $\mathcal{L}_X$  for loading  $X_i$  prepares the state  $\sqrt{1-p_i^0}|0\rangle + \sqrt{p_i^0}|1\rangle$ , so the probability for state  $|1\rangle$  encodes the default probability  $p_i^0$ .

Then we need to load the default correlation using operator  $\mathcal{L}_Z$ . The linear  $Y$ -rotation gate  $R_Y(z)$  for operator  $\mathcal{L}_Z$  satisfies that the probability for state  $|1\rangle$  would be  $p_i(z)$ . The expression for  $p_i(z)$  as a function of  $z$  and the correlation-free  $p_i$  just follows Eq.(2), which derives the slope and offset for the rotation gate for operator  $\mathcal{L}_Z$ , *i.e.*  $\sin^{-1}(\sqrt{p_i(z)}) = \text{slope} * z + \text{offset}$ . Meanwhile, we use  $n_z$  qubits to discretize the distribution to  $2^{n_z}$  slots, and use affine mapping<sup>12</sup> to encode the influence of  $z$  value in the quantum circuit. See derivation of slope and offset and explanation on affine mapping in Appendix II.

We need to note that the Gaussian or NIG distribution for systematic risk  $Z$  has to be loaded before operator  $\mathcal{L}_Z$ . The probability of  $z$ , *i.e.* the  $y$  axis of Gaussian distribution function, can be loaded using the built-in codes of uncertainty model in Qiskit, and we contribute the similar codes for NIG distribution.

Furthermore, we set an operator  $\mathcal{S}$  to sum up the loss due to all default events in this asset pool. The sum of loss equals to  $\sum a_i \lambda_i$ , where  $\lambda_i$  is the loss given default for asset  $i$ , and  $a_i$  is 1 if asset  $i$  default and is 0 vice versa. The probability for  $a_i = 1$  is just  $p_i(z)$  given by operator  $\mathcal{L}_Z$ . The maximum loss would be  $\sum \lambda_i$  when all assets default, so ensuring the maximum loss to be encoded needs  $n_s$  qubits that  $\sum \lambda_i \leq 2^{n_s} - 1$ . The operator  $\mathcal{S}$  uses  $2n_s$  qubits following the previous design of sum operator<sup>12</sup>. See Fig.2 for the quantum circuit framework for loading default events and summing up the loss.

## B. Calculate tranche loss

We use the comparator operator  $\mathcal{C}_{L_k}$  ( $k=1, 2$  and  $3$ ) to compare the sum of loss with the fixed lower attachment point  $K_{L_k}$  for each Tranche  $k$ . The comparator has been used to compare the underlying asset value with the striking price for option pricing in a recent work<sup>11</sup>, where the detailed quantum comparator circuit has been given.

The operator  $\mathcal{C}_{L_k}$  would flip a qubit from  $|0\rangle$  to  $|1\rangle$  if  $L(z)$ , the sum of loss under the systematic risk  $Z$ , is higher than  $K_{L_k}$ , and would keep  $|0\rangle$  otherwise. Meanwhile, the objective qubit will also rotate its state under the control of the comparator ancilla qubit. The piecewise linear rotation operator  $\mathcal{R}$  would then rotate  $\cos(g_0)|0\rangle + \sin(g_0)|1\rangle$  into:  $\sqrt{1-P_1}|0\rangle + \sqrt{P_1}|1\rangle$  (See Fig.2).  $g_0 = \frac{\pi}{4} - c$ , and  $c$  is a scaling factor. The setting ensures the probability after rotation remains in the monotonously increasing region when total loss increases.  $P_1$ , the probability at state  $|1\rangle$ , is found to have a relationship with the tranche loss:

$$P_1 = (\frac{1}{2} - c) + \frac{2c}{K_{U_k} - K_{L_k}}(\mathbb{E}[L_k]) \quad (4)$$

where  $\mathbb{E}[L_k]$  is the expectation of loss for a certain tranche  $k$ , for instance, the loss for Equity Tranche when setting  $K_{L_1}$  and  $K_{U_1}$ . See detailed derivation for Eq.(4) in Appendix III.

Then it comes to the issue how to read the value of  $P_1$ . We know that measuring an arbitrary state will make it collapse to the orthogonal basic state. Instead, Quantum Amplitude Estimation (QAE) would be able to map the amplitude to be estimated ( $P_1$  in this case) to the discretized value using  $m$  additional qubits, and hence read  $P_1$ . The QAE circuit involving controlled rotation gates and inverse quantum Fourier transform is explained in Appendix IV. QAE has been demonstrated as a good alternative to Monte Carlo simulation for finance pricing<sup>10-13</sup>. In this work, QAE that estimates  $P_1$  allows us to obtain the CDO tranche loss and return.

## III. RESULT ANALYSIS

We consider an example to show the pricing for CDO tranches. As listed in Table I, the CDO pool has four assets, each showing a default probability  $p_i^0$ , a sensitivity to the systematic risk  $\gamma_i$  and a loss given default  $\lambda_i$ .

The CDO is divided into three tranches: the Equity, Mezzanine and Senior Tranches. Values for the lower attachment point  $K_{L_k}$  and upper attachment point  $K_{U_k}$  for three tranches are provided in Table II.

For this task, we need  $n_x = 4$  qubits to represent the four assets in operator  $\mathcal{L}_X$ , and  $n_z = 4$  qubits in operator  $\mathcal{L}_Z$  to make  $2^4 = 16$  slots for the uncertainty distribution of systematic risk  $Z$ . We implement Gaussian (Fig.3a) and NIG (Fig.3b) distribution for  $Z$ .

For NIG distribution, by setting the parameters given in Appendix I, it shows a skewness of 1 and kurtosis

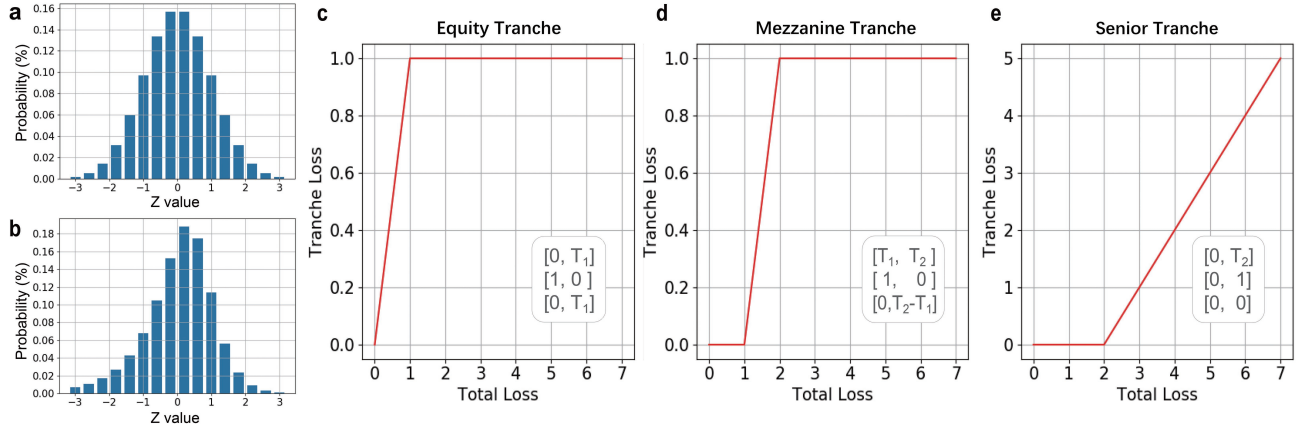


FIG. 3: **Systematic risk distribution and the tranche loss functions** (a-b) The probabilities of  $2^{n_z}$  different  $z$  values using  $n_z$  qubits follow the Gaussian distribution (mean=0, variance=1) in (a) and the NIG distribution (skewness=1, kurtosis=6, mean=0, variance=1) in (b). For both distributions, the range is from  $-3 \times \text{variance}$  to  $3 \times \text{variance}$ . (c-e) The tranche loss as a function of cumulative loss for (c) Equity Tranche, (d) Mezzanine Tranche, and (e) Senior Tranche. In the white box in (c-e), the first, second and third array respectively show the breakpoints, slopes and offsets for this tranche.  $T_1$  is the attachment point between Equity and Mezzanine Tranche, while  $T_2$  is that between Mezzanine and Senior Tranche.

of 6, which are consistent with a real CDO market<sup>25</sup>. Comparing with Gaussian distribution, this is narrower and centered to the left.

TABLE I: **The relevant parameters for each asset.**

Asset $i$	$\lambda_i$	$p_i^0$	$\gamma_i$
1	2	0.3	0.05
2	2	0.1	0.15
3	1	0.2	0.1
4	2	0.1	0.05

TABLE II: **The attachment points for each tranche.**

Tranche Name	Lower $K_{L_k}$	Upper $K_{U_k}$
Equity	0	1
Mezzanine	1	2
Senior	2	7

The step after loading distribution is to calculate the cumulative loss. The maximal loss is  $\sum \lambda_i = 7$  for this portfolio. Therefore, we can use  $n_s = 3$  qubits to encode the total loss in the weighted sum operator  $\mathcal{S}$ .

The pricing of the tranche loss is similar to the call option pricing, where there is a linear ‘payoff function’ that goes up from zero after the option striking price or, for the CDO tranche, the attachment point. The tranche loss as a function of the total cumulative loss is given in Fig.3c-e for this specific example. See Appendix V for how to set the input parameters (*e.g.*, ‘breakpoint’) for the piecewise linear rotation function.

We then use QAE to estimate  $P_1$  and convert it to the tranche loss according to Eq.(4). We use the QASM cloud backend that is in the Noisy Intermediate-Scale Quantum (NISQ) environment. Fig.4 demonstrates the calculated tranche loss for an NIG distribution (Fig.3b) using quantum computation with  $m = 4$  qubits in QAE and the classical Monte Carlo method. The results from the two approaches match well. When  $z$  follows Gaussian distribution (Fig.3a), consistent results have also been obtained, as shown in Fig. A2 in the appendix.

With the calculated tranche loss, we can price the CDO tranche return according to Eq.(1). The notional value  $N$  for the Equity Tranche, Mezzanine Tranche and Senior Tranche is 1, 1, and 5, respectively, by calculating  $K_U - K_L$  for each tranche. We get the tranche loss from quantum computation and calculate the tranche return for Equity, Mezzanine and Senior Tranche to be 49.9%, 48.1% and 1.8%. The low return for the Senior Tranche is consistent with the practice in reality. Such a low value is firstly due to the last sequence to bear the loss, and secondly owing to its large notional value, which is normally above 80% of the sum for the three tranches. See more discussion on tranche return in practice in Appendix VI.

#### IV. DISCUSSION AND CONCLUSION

The CDO is a relatively advanced and complex structured finance product, and the credit market plays a significant role in the finance industry. Therefore, despite there were some disputes on CDOs during the 2008 financial crisis, CDOs are still widely studied products in quantitative finance, and are being improved with various financial models. In this work, we implement the normal inverse Gaussian model that is now regarded as advantageous over the Gaussian model. There is also the

variance gamma model that was first applied to option pricing<sup>31</sup> and later found to be a good model for CDO pricing<sup>32</sup>. Such improved models can also be calculated via quantum computation.

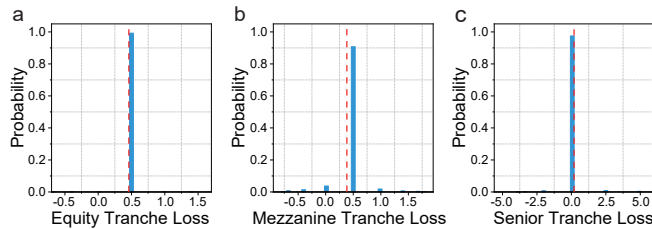


FIG. 4: **CDO tranche loss with  $Z$  under the NIG distribution.** The calculated loss for (a) Equity Tranche, (b) Mezzanine Tranche, and (c) Senior Tranche.  $Z$  follows the NIG distribution depicted in Fig.3b. Blue bars indicate quantum computation results with  $m = 4$  for QAE, and red dashed lines indicate Monte Carlo results with repeating 10000 times.

Note that the quantum adaption of generative adversarial network<sup>7,16</sup> has now been considered as an effective way to load any distribution in quantum circuits<sup>15</sup> and can be applied to more finance models. Besides, the parameter shift rule<sup>33,34</sup> has been raised to solve the issue of encoding gradients in quantum circuits, which facilitates the mapping of machine learning techniques in quantum algorithms. Furthermore, the trendy variational quantum algorithms that are suitable for NISQ environment, and the alternative approach using quantum annealing<sup>35</sup>, may work on a large variety of optimization tasks in fi-

nance. In all, there's much room to explore for quantum computation in finance applications.

## Acknowledgments

H.T. thanks Prof. Stephen Schaefer's previous help for studies on fixed income and interest rate derivative at London Business School. The authors thank Jian-Wei Pan for helpful discussions. This research was supported by National Key R&D Program of China (2019YFA0308700, 2017YFA0303700), National Natural Science Foundation of China (61734005, 11761141014, 11690033, 11904229), Science and Technology Commission of Shanghai Municipality (STCSM) (17JC1400403), and Shanghai Municipal Education Commission (SMEC) (2017-01-07-00-02- E00049). X.-M.J. acknowledges additional support from a Shanghai talent program.

**Author Contributions.** H.T. and X.-M.J. conceived and supervised the project. H.T. and A.P. designed the scheme. A.P. wrote the Qiskit code. H.T. did Monte Carlo simulation. H.T., A.P., L.F.Q., T.Y.W., J.G. and X.M.J. analyzed the data and presented the figures. H.T. wrote the paper, including the appendix, with input from all the other authors. **Competing Interests.** The authors declare no competing interests. **Data Availability.** The data that support the plots within this paper and other findings of this study are available from the corresponding author upon reasonable request.

\* Electronic address: htang2015@sjtu.edu.cn

† Electronic address: xianmin.jin@sjtu.edu.cn

- Orús, R., Mugel, S., & Lizaso, E. Quantum computing for finance: Overview and prospects. *Rev. in Phys.* **4**, 100028 (2019).
- Baaquie, B. E. *Quantum finance: Path integrals and Hamiltonians for options and interest rates*. Cambridge University Press (2007).
- Zhang, C., & Huang, L. A quantum model for the stock market. *Physica A: Statistical Mechanics and its Applications* **389**, 5769-5775 (2010).
- Meng, X., Zhang, J. W., & Guo, H. Quantum Brownian motion model for the stock market. *Physica A: Statistical Mechanics and its Applications* **452**, 281-288 (2016).
- Brassard, G., Hoyer, P., Mosca, M., & A. Tapp, A. Quantum Amplitude Amplification and Estimation. *Contemporary Mathematics* **305**, 53-74 (2002).
- Lloyd, S., Mohseni, M., & Rebentrost, P. Quantum principal component analysis. *Nat. Phys.* **10**, 631-633 (2014).
- Lloyd, S., & Weedbrook, C. Quantum Generative Adversarial Learning. *Phys. Rev. Lett.* **121**, 040502 (2018).
- Peruzzo, A., McClean, J., Shadbolt, P., Yung, M.-H., Zhou, X.-Q., Love, P. J., Aspuru-Guzik, A., & O'Brien, J. L. A variational eigenvalue solver on a quantum processor. *Nat. Commun.* **5**, 4213 (2014).

- Farhi, E., Goldstone, J., & Gutmann, S. A Quantum Approximate Optimization Algorithm. *arXiv Preprint arXiv:1411.4028* (2014).
- Rebentrost, P., Gupt, B., & Bromley, T. B. Quantum computational finance: Monte Carlo pricing of financial derivatives. *Phys. Rev. A* **98**, 022321 (2018).
- Stamatopoulos, N., Egger, D. J., Sun, Y., Zoufal, C., Iten, R., Shen, N., & Woerner, S. Option Pricing using Quantum Computers. *Quantum* **4**, 291 (2020).
- Egger, D. J., Gutiérrez, R. G., Mestre, J. C., & Woerner, S. Credit Risk Analysis using Quantum Computers. *arXiv Preprint arXiv:1907.03044* (2019).
- Woerner, S., & Egger, D. J. Quantum risk analysis. *npj Quantum Info.* **5**, 15 (2019).
- Martin, A., Candelas, B., Rodríguez-Rozas, A., Martín-Guerrero, J. D., Chen, X., Lamata, L., Orús, R., Solano, E., & Sanz, M., Towards Pricing Financial Derivatives with an IBM Quantum Computer. *arXiv Preprint arXiv:1904.05803* (2019).
- Zoufal, C., Lucchi, A., & Woerner, S. Quantum Generative Adversarial Network for Learning and Loading Random Distributions. *npj Quantum Info.* **5**, 103 (2019).
- Goodfellow, I. J., Pouget-Abadie, J., Mirza, M., Xu, B., Warde-Farley, D., Ozair, S., Courville, A., & Bengio, Y. Generative Adversarial Nets. *Conference proceedings of*



- advances in neural information processing systems* 2672-2680 (2014).
17. Hull, J. C. *Options futures and other derivatives*. Pearson Education India (2003).
  18. Tuckman, B., & Serrat, A. *Fixed income securities: tools for today's markets, 3rd Edition*. John Wiley & Sons (2012).
  19. Chacko, G., Sjöman, A., Motohashi, H., & Dessain, V. *Credit Derivatives, Revised Edition: A Primer on Credit Risk, Modeling, and Instruments*. Pearson Education (2016).
  20. Black, F. & Scholes, M. The pricing of options and corporate liabilities. *J. Political Econ.* **81**, 637-654 (1973).
  21. Merton, R.C. Theory of rational option pricing. *The Bell Journal of economics and management science* **4**, 141-183 (1973).
  22. Li, D. X. On default correlation: A copula function approach. *The Journal of Fixed Income* **9**, 43-54 (2000).
  23. Barndorff-Nielsen, O. Hyperbolic Distributions and Distributions on Hyperbolae. *Scandinavian Journal of Statistics* **5**, 151-157 (1978).
  24. Barndorff-Nielsen, O. Normal Inverse Gaussian Distributions and Stochastic Volatility Modelling. *Scandinavian Journal of Statistics* **24**, 1-13 (1997).
  25. Guégan, D., & Houdain, J. Collateralized Debt Obligations pricing and factor models: a new methodology using Normal Inverse Gaussian distributions. Note de Recherche IDHE-MORA No. 007-2005, ENS Cachan. (2005).
  26. Kalemanna, A., Schmid, B., & Werner, R. The Normal Inverse Gaussian distribution for Synthetic CDO Pricing. *The Journal of Derivatives* **Spring**, 80-93 (2007).
  27. Schlösser, A. Normal Inverse Gaussian Factor Copula Model. *Pricing and Risk Management of Synthetic CDOs* 80-93, Springer Berlin (2011).
  28. Rutkowski, M., & Tarca, S. Regulatory Capital Modelling for Credit Risk. *International Journal of Theoretical & Applied Finance* **18**, 5 (2014).
  29. Vašíček, O. Probability of loss on loan portfolio. *Technical report, KMV Corporation* (1987).
  30. Vašíček, O. The distribution of loan portfolio value. *Risk* **15**, 160-162 (2002).
  31. Madan, D. B., Carr, P. P., & Chang, E. C. The Variance Gamma Process and Option Pricing. *European Finance Review* **2**, 79-105 (1998).
  32. Moosbrucker, T. Pricing CDOs with Correlated Variance Gamma Distributions. working paper, Centre for Financial Research, University of Cologne. (2006).
  33. Li, J., Yang, X. D., Peng, X. H., & Sun, C. P. Hybrid quantum-classical approach to quantum optimal control. *Phys. Rev. Lett.* **118**, 150503 (2017).
  34. Schuld, M., Bergholm, V., Gogolin, C., Izaac, J., & Killoran, N. Evaluating analytic gradients on quantum hardware. *Phys. Rev. A* **99**, 032331 (2019).
  35. Cohen, J., Khan, A., & Alexander, C. Portfolio Optimization of 40 Stocks Using the DWave Quantum Annealer. *arXiv Preprint arXiv: 2007.01430* (2020).

## Appendix I The model of Normal Inverse Gaussian Distribution

The Normal Inverse Gaussian (NIG) distribution mixes the normal Gaussian distribution and inverse Gaussian distributions[Ref A1].

The word ‘inverse’ in the name needs to be explained. While normal distribution reflects the location distribution under Brownian motion at a certain time, the inverse Gaussian distribution shows the time distribution when the Brownian motion moves to a certain location, so inverse suggests an inverse way in viewing location and time.

Firstly, for a random variable  $Y$  that has inverse Gaussian distribution, its density of function is of the form:

$$f_{IG}(y; \alpha, \beta) = \frac{\alpha}{\sqrt{2\pi}\beta} y^{-3/2} \exp\left(-\frac{(\alpha - \beta y)^2}{2\beta y}\right) \quad (A1)$$

Then if a random variable  $X$  satisfies the following requirement with parameters  $\alpha$ ,  $\beta$ ,  $\mu$  and  $\delta$ , it follows the Normal Inverse Gaussian distribution  $\mathcal{NIG}(x; \alpha, \beta, \mu, \delta)$ :

$$\begin{aligned} X|Y = y &\sim \mathcal{N}(\mu + \beta y, y) \\ Y &\sim \mathcal{IG}(\gamma, \gamma^2) \text{ with } \gamma = \sqrt{\alpha^2 - \beta^2} \end{aligned} \quad (A2)$$

The full expression of the probability density function for NIG distribution is a bit complicated:

$$\begin{aligned} \mathcal{NIG}(x; \alpha, \beta, \mu, \delta) &= \\ a(\alpha, \beta, \mu, \delta) q\left(\frac{x - \mu}{\delta}\right)^{-1} K_1\left(\delta \alpha q\left(\frac{x - \mu}{\delta}\right)\right) e^{\beta x} \end{aligned} \quad (A3)$$

where the function  $q$  follows:  $q(x) = \sqrt{1 + x^2}$ , and  $a$  is the function with variables  $\alpha$ ,  $\beta$ ,  $\mu$  and  $\delta$ :

$$a(\alpha, \beta, \mu, \delta) = \pi^{-1} \alpha \exp(\delta \sqrt{\alpha^2 - \beta^2 - \beta \mu}) \quad (A4)$$

with parameters satisfying:  $0 < |\beta| < \alpha$  and  $\delta > 0$ , and  $K_1$  is the first index of the Bessel function of the third kind:

$$K_1(x) = x \int_1^\infty \exp(-xt) \sqrt{t^2 - 1} dt \quad (A5)$$

The parameter  $\alpha$  is related to steepness,  $\beta$  to symmetry,  $\mu$  to location and  $\delta$  to scale. In order to realize the NIG distribution (mean=0, variance=1, skewness=1, and kurtosis=6), the parameters need to be set as follows[Ref A2]:  $\alpha = -1.6771$ ,  $\beta = 0.75$ ,  $\mu = -0.6$ , and  $\delta = 1.2$ .

It's worth noting that despite of the complexity of NIG distribution functions, they can be conveniently implemented using the built-in functions in Scipy. We then write the uncertainty model and conditional independence model for the NIG distribution and contribute it to the Qiskit package, in the same folder with those for the Gaussian distribution (`\qiskit\aquas\components\uncertainty_models`).

## Appendix II Derive the linear rotation parameters for operator $\mathcal{L}_Z$ and explain affine mapping

A linear rotation function would use the state qubit  $|x\rangle$  to work on the target qubit  $|0\rangle$ :

$$\begin{aligned} |x\rangle |0\rangle &\rightarrow |x\rangle (\cos(\text{slope} * x + \text{offset}) |0\rangle \\ &\quad + \sin(\text{slope} * x + \text{offset}) |1\rangle) \end{aligned} \quad (A6)$$

After the rotation, the probability at the state  $|1\rangle$  would be the probability that we are interested in, and it is the  $z$ -tuned default probability  $p_i(z)$  in operator  $\mathcal{L}_Z$ :

$$\sqrt{p_i(z)} = \sin(\text{slope} * z + \text{offset}) \quad (A7)$$

so  $\sin^{-1} \sqrt{p_i(z)}$  has to be expressed in the form of  $\text{slope} * z + \text{offset}$  to get the  $\text{slope}$  and  $\text{offset}$  for the linear rotation quantum gate in operator  $\mathcal{L}_Z$ .

Combining the expression for  $p_i(z)$  in Eq.(2) using the conditional independence model, we have:

$$\sin^{-1} \sqrt{p_i(z)} = \sin^{-1} \sqrt{F\left(\frac{F^{-1}(p_i^0) - \sqrt{\gamma_i} z}{\sqrt{1 - \gamma_i}}\right)} \quad (A8)$$

where  $F$  is the cumulative distribution function (CDF), and we denote  $\psi = \frac{F^{-1}(p_i^0)}{\sqrt{1-\gamma_i}}$ , so the above equation can be simply expressed as:

$$\sin^{-1}\sqrt{p_i(z)} = \sin^{-1}\sqrt{F(\psi - \frac{\sqrt{\gamma_i}z}{\sqrt{1-\gamma_i}})} \quad (\text{A9})$$

The first order Taylor's theorem can be expressed as:

$$g(x) = g(a) + g'(a)(x - a) \quad (\text{A10})$$

where  $g'(a)$  is the first derivative of the function  $g(x)$ .

Now let  $x$  be  $\psi - \frac{\sqrt{\gamma_i}z}{\sqrt{1-\gamma_i}}$ , and  $a$  be  $\psi$ , then  $x - a$  is  $-\frac{\sqrt{\gamma_i}z}{\sqrt{1-\gamma_i}}$ . We know that for Taylor expansion,  $x - a$  has to be a very marginal value.  $\frac{\sqrt{\gamma_i}z}{\sqrt{1-\gamma_i}}$  satisfies this. From the example given in the Result Analysis Section,  $\gamma$  is generally below 0.2 and  $z$  follows a Gaussian or NIG distribution, ranging between  $[-1, 1]$  with a value close to zero at most times. Therefore, Taylor's theorem for this task is reasonable.

In this scenario, function  $g(x)$  is  $\sin^{-1}\sqrt{F(x)}$ . It is a composite function, so the chain rule should be considered for the derivative function  $g'(a)$ .  $\sin^{-1}(h)' = \frac{1}{\sqrt{1-h^2}}$  and  $(\sqrt{h})' = \frac{1}{2\sqrt{h}}$  apply for any variable  $h$ , and note that  $F$  is the cumulative distribution function (CDF), the derivative of  $F$  would just be the probability density function (pdf) which is normally denoted as  $f$ . Now  $g'(a)$  reads:

$$g'(a) = \frac{-f(\psi)}{2\sqrt{1-F(\psi)}\sqrt{F(\psi)}} \quad (\text{A11})$$

Therefore we get:

$$\begin{aligned} & \sin^{-1}\sqrt{F(\psi - \frac{\sqrt{\gamma_i}z}{\sqrt{1-\gamma_i}})} = \\ & \sin^{-1}\sqrt{F(\psi)} + \frac{-f(\psi)}{2\sqrt{1-F(\psi)}\sqrt{F(\psi)}} \frac{\sqrt{\gamma_i}z}{\sqrt{1-\gamma_i}} \end{aligned} \quad (\text{A12})$$

One can now very easily get the expression for *slope* and *offset*:

$$\text{slope} = \frac{-\sqrt{\gamma_i}}{2\sqrt{1-\gamma_i}} \frac{f(\psi)}{\sqrt{1-F(\psi)}\sqrt{F(\psi)}} \quad (\text{A13})$$

$$\text{offset} = 2\arcsin(\sqrt{F(\psi)}) \quad (\text{A14})$$

In the  $\mathcal{L}_Z$  operator, with  $n_z$  qubits, we can truncate and discretize the distribution to  $2^{n_z}$  slots. For instance, with 3 qubits,  $z$  ranges between 0 and 7 that corresponds to  $-3\sigma$  to  $3\sigma$  of the Gaussian distribution; for  $z = 4 = 1 * 2^0 + 0 * 2^1 + 1 * 2^2 - 1$ , Qubit 1 and Qubit 3 turn on their controlled rotation gate  $R_Y(2^0)$  and  $R_Y(2^2)$ , while Qubit 2 does not switch on its  $R_Y(2^1)$ . Through such a so-called affine mapping[Ref A3], the influence of  $z$  value on the linear rotation is encoded in the quantum circuit.

### Appendix III Piecewise linear rotation for objective qubit

We use the comparator operator  $\mathcal{C}_{L_k}$  ( $k=1, 2$  and  $3$ ) to compare the sum of loss with the fixed lower attachment point  $K_{L_k}$  for each Tranche  $k$ . The comparator has been used to compare the underlying asset value with the striking price for option pricing in a recent work[Ref A4], where the detailed quantum comparator circuit has been given.

The operator  $\mathcal{C}_{L_k}$  would flip a qubit from  $|0\rangle$  to  $|1\rangle$  if  $L(z)$ , the sum of loss under the systematic risk  $Z$ , is higher than  $K_{L_k}$ , and would keep  $|0\rangle$  otherwise. For simplicity, we just discuss  $\mathcal{C}_L$  generally that can later apply to all  $\mathcal{C}_{L_k}$ s by just setting  $K_L$  to  $K_{L_k}$ .

Meanwhile, the objective qubit will also rotate its state under the control of the comparator ancilla qubit. The comparator  $\mathcal{C}_L$  and a piecewise linear rotation operator  $\mathcal{R}$  map  $|\psi\rangle|0\rangle[\cos(g_0)|0\rangle + \sin(g_0)|1\rangle]$  into:

$$\begin{cases} |\psi\rangle|0\rangle[\cos(g_0)|0\rangle + \sin(g_0)|1\rangle] & \text{if } L(z) \leq K_L \\ |\psi\rangle|1\rangle[\cos(g_0 + g_z)|0\rangle + \sin(g_0 + g_z)|1\rangle] & \text{if } L(z) > K_L \end{cases} \quad (\text{A15})$$



and the probability at state  $|1\rangle$  that can be measured using QAE would be expressed as follows:

$$P_1 = \sum_{L(z) \leq K_L} f(z) \sin^2(g_0) + \sum_{L(z) > K_L} f(z) \sin^2(g_0 + g_z) \quad (\text{A16})$$

where  $f(z)$  shows the probability of a systematic risk value  $z$  distributed following a certain probability density function  $f$ .  $g_0$  is set to be  $\frac{\pi}{4} - c$ .  $g_z$  is a linear function that contains the total loss  $L(z)$  and scaling factor  $c$ .  $g_z$  can be implemented using controlled  $Y$ -rotations, and it's mapped to integer value  $z \in \{0, \dots, 2^{n_z} - 1\}$ . Note that there is an upperbound breakpoint  $K_U$  as well, so we set another comparator operator  $\mathcal{C}_U$  that encodes  $K_U$ , and  $g_z$  finally reads as:

$$g_z = 2c \frac{\min(L(z), K_U) - K_L}{K_U - K_L} \quad (\text{A17})$$

With such settings  $g_z$  would be in the range  $\{0, 2c\}$ , and by choosing a small scaling parameter  $c$ , we can ensure  $\sin(g_0 + g_z)$  in a monotonously increasing regime. Given that for marginal  $x$ :  $\sin^2(x + \frac{\pi}{4}) = x + \frac{1}{2} + \mathcal{O}(x^3)$ , the expression for probability  $P_1$  can be further derived:

$$\begin{aligned} P_1 &= \sum_{L(z) \leq K_L} f(z) \left(\frac{1}{2} - c\right) + \\ &\quad \sum_{L(z) > K_L} f(z) \left(\frac{1}{2} - c + 2c \frac{\min(L(z), K_U) - K_L}{K_U - K_L}\right) \\ &= \left(\frac{1}{2} - c\right) + \sum_{L(z) > K_L} f(z) \left(2c \frac{\min(L(z), K_U) - K_L}{K_U - K_L}\right) \\ &= \left(\frac{1}{2} - c\right) + \frac{2c}{K_U - K_L} (\mathbb{E}[L_{tranche}]) \end{aligned} \quad (\text{A18})$$

where  $\mathbb{E}[L_{tranche}]$  is the expectation of loss for a certain tranche, for instance, setting  $K_L$  and  $K_U$  to be  $K_{L_1}$  and  $K_{U_1}$ , we get the loss for the Equity Tranche. Therefore, when we have obtained  $P_1$  from the QAE circuit, we would be able to get the tranche loss and return.

#### Appendix IV Quantum Amplitude Estimation

Given a Boolean function  $f$ : to find an  $x \in X$  where  $X \rightarrow \{0, 1\}$  such that  $f(x) = 1$ , we can denote  $N$  as the number of inputs on which  $f$  takes the value 1, and it can be written as  $N = |\{x \in (X) | f(x) = 1\}|$ .

If we have a classical probabilistic algorithm  $P$  that outputs a guess on input  $x$ , the solution to instance  $x$  can be found by repeatedly calling  $P$  and  $X$ . If  $X(x, P(x)) = 1$  with probability  $p > 0$ , we have to repeat the process  $\frac{1}{p}$  times on average.

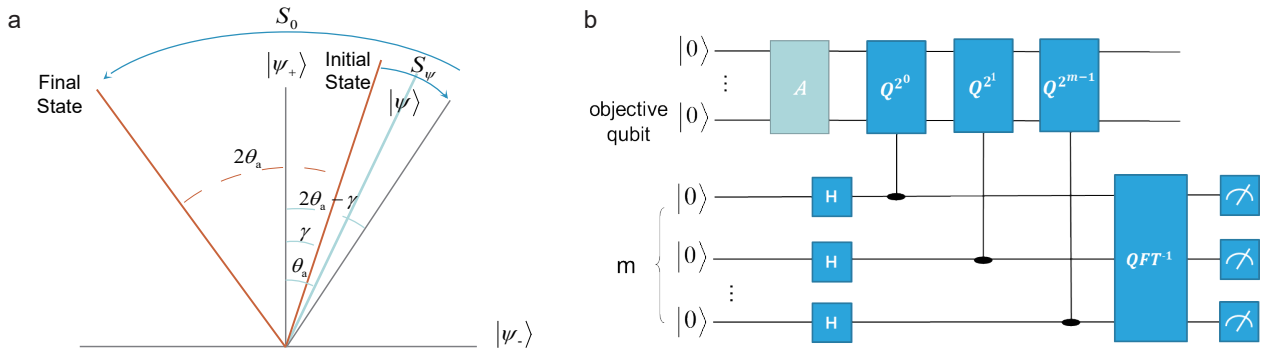


FIG. A1: **Theoretical framework for QAE.** (a) Illustration for angle rotation by operator  $Q$ . (b) The quantum circuit for quantum phase estimation.  $H$  denotes the Hadamard gate.  $QFT^{-1}$  denotes the inverse quantum Fourier transform.

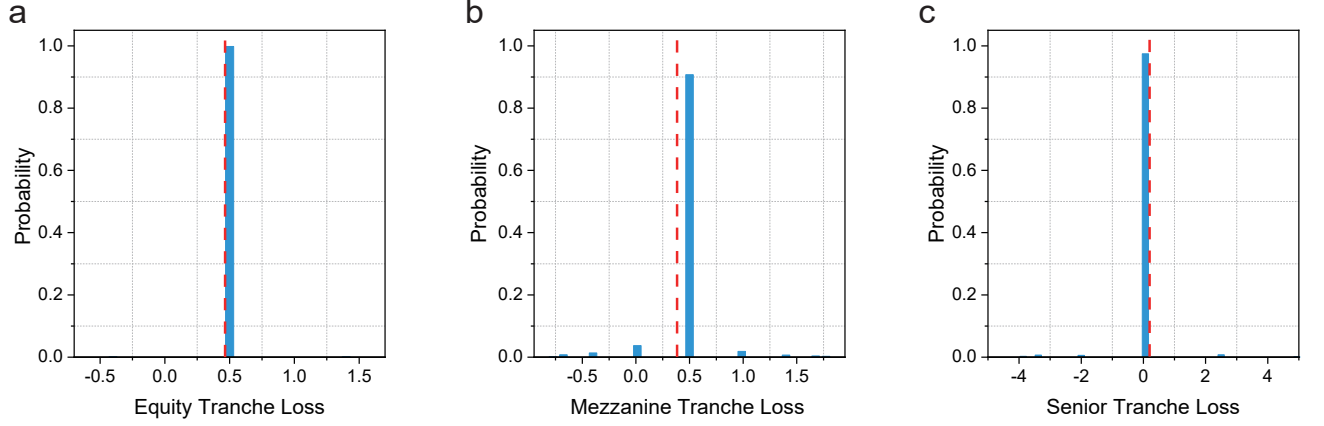


FIG. A2: **CDO tranche loss with  $Z$  under the Gaussian distribution.** The calculated loss for (a) the Equity Tranche, (b) the Mezzanine Tranche, and (c) the Senior Tranche. The systematic risk  $Z$  follows the Gaussian distribution (mean=0, variance=1). Blue bars indicate the results from quantum computation with  $m = 4$  for QAE, and red dashed lines indicate the Monte Carlo results with repeating 10000 times.

Suppose given a unitary transformation,  $\mathcal{A}$ , which is a quantum algorithm, unlike making measurement in the case of classical  $P$  algorithm, this produces a quantum superposition state of the “desired” result that  $X(x, P(x)) = 1$  and “undesired” result that  $X(x, P(x)) \neq 1$ . Then amplitude estimation is the problem of estimating  $a$ , the probability that a measurement of  $|\psi\rangle$  yields a good solution. It is sufficient to evaluate  $\mathcal{A}$  and  $X$  in an expected number of times that is proportional to  $\frac{1}{\sqrt{a}}$ .

To explain amplitude estimation, the quantum state after unitary transformation  $\mathcal{A}$  can be expressed as a linear combination of  $\psi_+$  and the orthogonal  $\psi_-$ :

$$\mathcal{A}|0\rangle = |\psi\rangle = -\frac{i}{\sqrt{2}} (e^{i\theta_a} |\psi_+\rangle + e^{-i\theta_a} |\psi_-\rangle) \quad (\text{A19})$$

so the success probability “ $a$ ” is converted to the solution of angle  $\theta_a$  that decides the eigenvalue for unitary transformation  $\mathcal{A}$ .

Apply an operator  $Q$  to  $\mathcal{A}$ :

$$Q = AS_0A^\dagger S_{\psi_0} \quad (\text{A20})$$

where  $S_0 = 1 - 2|0\rangle\langle 0|$ , and  $S_{\psi_0} = 1 - 2|\psi\rangle\langle 0|0\rangle\langle\psi|$ . As illustrated in Fig.A1a, an initial state first rotates along  $\psi$  by the operator  $S_{\psi_0}$ , and then rotates along  $\psi_+$  by the operator  $S_0$ . Therefore, the angle between the arbitrarily set initial state and the final state after the operator  $Q$  becomes  $2\theta_a$ . In this case when the initial state is  $\mathcal{A}$ , operator  $Q$  just shifts from  $|\psi\rangle$  for  $2\theta_a$ .

The task of finding the eigenvalue for quantum state  $|\psi\rangle$  of the unitary transformation  $\mathcal{A}$  can be fulfilled by Quantum Phase Estimation that requires another register with  $m$  additional qubits. As shown in Fig.A1b, the phase estimation quantum circuit comprises Hadamard gates, controlled-rotation operators and an inverse quantum Fourier transform ( $QFT^{-1}$ ) operation.

Firstly, the Hamamard gates prepare the  $m$  qubits in the uniform superposition:

$$|0\rangle^{\otimes m} |\psi\rangle \rightarrow \frac{1}{\sqrt{2^m}} \sum_{j=0}^{2^m-1} |j\rangle |\psi\rangle \quad (\text{A21})$$

As has been mentioned, the operator  $Q$  essentially causes a Y-rotation of angle  $2\theta_a$ , i.e.,  $Q = R_y(2\theta_a)$ . In this phase estimation circuit, the many controlled-rotation operators  $Q_j$  satisfies:  $Q_j = R_y(2j\theta_a)$ , and they turn the above Eq. (A21) into:

$$\frac{1}{\sqrt{2^m}} \sum_{j=0}^{2^m-1} e^{2i\theta_a j} |j\rangle |\psi\rangle \quad (\text{A22})$$

Applying the  $\mathcal{QFT}^{-1}$  operation, we can reverse the action on vector  $|j\rangle$  to that on  $|\theta_a\rangle$ :

$$\mathcal{QFT}^{-1}\left(\frac{1}{\sqrt{2^m}} \sum_{j=0}^{2^m-1} e^{2i\theta_a j} |j\rangle |\psi\rangle\right) = \frac{1}{\pi} |\theta_a\rangle |\psi\rangle \quad (\text{A23})$$

By taking measurement on the register of  $m$  qubits, we can get the approximation of  $\theta_a$ . This is done by obtaining the measured integer  $y \rightarrow \{0, 1, 2, \dots, 2^m - 1\}$ . Taking  $M = 2^m$ , then  $\theta_a$  can be approximated as  $\tilde{\theta}_a = y\pi/M$ , which yields  $\tilde{a}$ , the approximation of the aforementioned probability  $a$ :

$$\tilde{a} = \sin^2\left(\frac{y\pi}{M}\right) \in [0, 1] \quad (\text{A24})$$

satisfying the following inequality:

$$|a - \tilde{a}| \leq \frac{\pi}{M} + \frac{\pi^2}{M^2} = O(M^{-1}) \quad (\text{A25})$$

with probability at least  $\frac{8}{M^2}$ . Comparing with the  $O(M^{-\frac{1}{2}})$  convergence rate of the classical Monte Carlo method, the quantum amplitude estimation method converges faster with a quadratic speed-up.

## Appendix V Set input parameters for the built-in piecewise linear rotation function in Qiskit

For the  $\mathcal{C}\&\mathcal{R}$  part of the quantum circuit shown in Fig.2 of the main text, we can use the built-in code named ‘PwlObjective’ for piecewise linear rotation function that includes the comparator  $\mathcal{C}$ , and the piecewise linear rotator  $\mathcal{R}$ . The built-in function uses the ‘breakpoints’ array to record the attachment points, and uses the ‘slopes’ and ‘offsets’ arrays in which slope  $k$  and offset  $k$  correspond to these for the line segment between breakpoint  $k - 1$  and breakpoint  $k$ . Note the offset is the  $y$ -axis value for the starting point of the line segment, instead of the intercept by extending the line segment to the  $y$  axis. The breakpoints, slopes and offsets for the tranche loss function are shown in each figure in Fig. 3c-e, which can be very straightforwardly calculated. These are used as the input parameters for the built-in piecewise linear rotation function.

## Appendix VI Discussion on tranche return in reality

It’s worth noting that the returns for Equity and Mezzanine Tranche in the case study of the main text are a bit too high, comparing to the custom returns that would be around 15-25% and 5-15% for the Equity and Mezzanine Tranche, respectively[Ref A5]. It’s partially because that default probabilities  $p_i$ s are a bit high. One more reason is that we ignore the recovery rate of the asset in order to focus on the essential structure. The recovery rate  $\eta$ , which is generally set as 40%, means that when asset defaults, some values can be recovered by ways like selling real estates to get funds to compensate investors. Then the maximum loss would equal to the total notional value multiplies  $(1-\eta)$ . In this example, the loss given default  $\lambda_1$  to  $\lambda_4$  would become 1.2, 1.2, 0.6 and 1.2, while the tranche attachment points keep unchanged. This would bring down the tranche loss.

## Supplementary References

- [A1] Schlösser, A. Normal Inverse Gaussian Factor Copula Model. *Normal Inverse Gaussian Factor Copula Model*. 80-93, Springer Berlin (2011).
- [A2] Guégan, D., & Houdain, J. Collateralized Debt Obligations pricing and factor models: a new methodology using Normal Inverse Gaussian distributions. Note de Recherche IDHE-MORA No. 007-2005, ENS Cachan (2005).
- [A3] Egger, D. J., Gutiérrez, R. G., Mestre, J. C., & Woerner, S. Credit Risk Analysis using Quantum Computers. *arXiv Preprint*, arXiv:1907.03044 (2019).
- [A4] Stamatopoulos, N., Egger, D. J., Sun, Y., Zoufal, C., Iten, R., Shen, N., & Woerner, S. Option Pricing using Quantum Computers. *Quantum* **4**, 291 (2019).
- [A5] Chacko, G., Sjöman, A., Motohashi, H., & Dessain, V. *Credit Derivatives, Revised Edition: A Primer on Credit Risk, Modeling, and Instruments*. Pearson Education (2016).